UCRL-91639
PREPRINT
CONF-850671--4

BLAST INDUCED SUBSIDENCE IN THE CRATERS OF NUCLEAR TESTS OVER CORAL

Donald E. Burton
Robert P. Swift
H. David Glenn
Jon B. Bryan

This paper has been prepared for presentation to the 26th U.S. Symposium on Rock Mechanics, to be held at Rapid City, South Dakota, June 26-28, 1985.

February, 1985

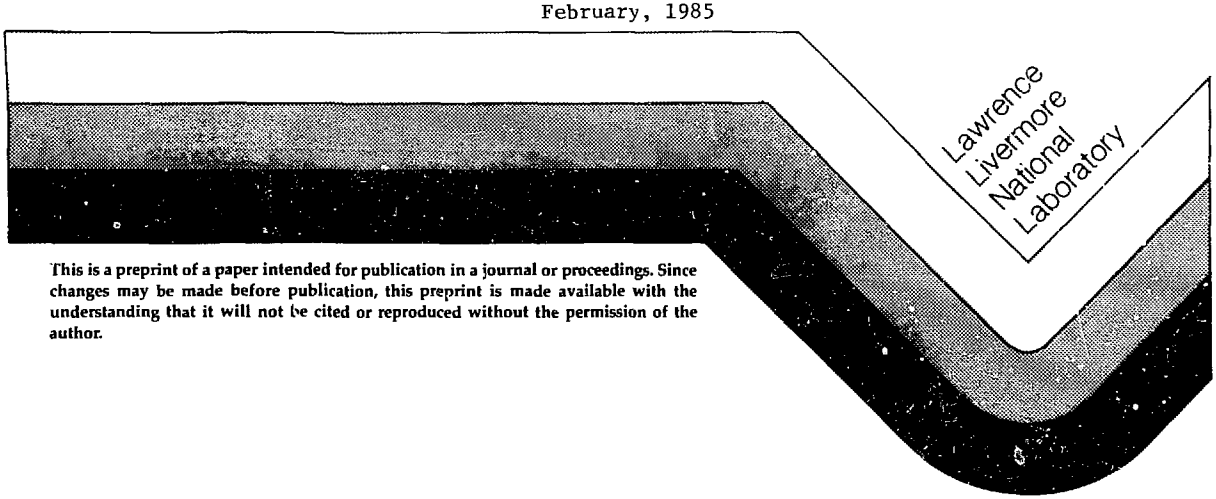

Blast induced subsidence in the craters of nuclear tests over coral*

Donald E. Burton, Robert P. Swift, H. David Glenn, Jon B. Bryan,
Lawrence Livermore National Laboratory, Livermore, CA 94550

DISCLAIMER

UCRL--91639

DE85 007975

ABSTRACT

The craters from high-yield nuclear tests at the Pacific Proving Grounds are very broad and shallow in comparison with the bowl-shaped craters formed in continental rock at the Nevada Test Site and elsewhere. Attempts to account for the differences quantitatively have been generally unsatisfactory.

We have for the first time successfully modeled the Koa Event, a representative coral-atoll test. On the basis of plausible assumptions about the geology and about the constitutive relations for coral, we have shown that the size and shape of the Koa crater can be accounted for by subsidence and liquefaction phenomena. If future studies confirm these assumptions, it will mean that some scaling formulas based on data from the Pacific will have to be revised to avoid overestimating weapons effects in continental geology.

1. INTRODUCTION

To understand the effectiveness of nuclear weapons, one must be able to predict the effects of near-surface detonations of relatively high-yield nuclear devices (several hundred kilotons) on targets embedded in various kinds of rocks and soils. However, all of the high-yield explosive cratering events in the U.S. data base took place at the Pacific Proving Grounds (PPG). The PPG are located at the Enewetak and Bikini atolls. The geology of these coral atolls is unlike that of any continent. The matter is not academic; empirical formulas used until recently to predict the size and shape of weapon craters [Cooper 1977] are based on data from the PPG. We now believe that these formulas greatly over-estimate surface-burst effectiveness in typical continental geologies.

There have been so few above-ground and shallow-buried nuclear events that it has been necessary to develop numerical techniques to extrapolate beyond known craters to predict the effects of new weapons and new geologic settings. Some doubt remains about the completeness of such models because of their inability to reproduce the very shallow, saucer-shaped craters formed in coral at the PPG. Calculated crater volumes in studies by some investigators are only about 20 to 25% of those

*This work was performed under the auspices of U.S. Department of Energy by Lawrence Livermore National Laboratory under contract No. W-7405-Eng-48.

observed in coral, and none have reproduced the shapes associated with these events. For example, Figure 1 contrasts the result of a typical numerical simulation [Schuster 1983] with the profile of the Koa event crater [Ristvet 1978] which has a volume of 2.11×10^7 m^3 and radius of about 600 m.

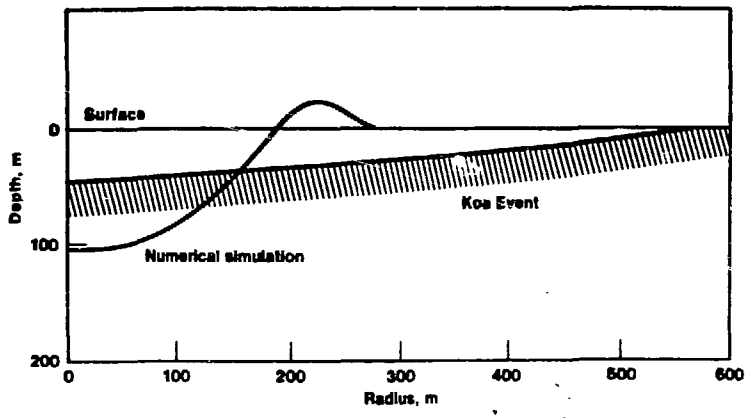

Figure 1. Profile of a Pacific Proving Ground Crater (Koa Event) contrasted with the crater resulting from a typical numerical simulation (Schuster 1983).

Various physical mechanisms have been postulated for the size and shape of the Pacific craters. In this work, we have developed a multiphase constitutive model based on mixture theory [Swift 1984], introduced it into our two-dimensional continuum dynamics code TENSOR [Burton 1977, 1982], and applied it to a simulation of the Koa Event. Our studies [Burton 1984] attribute the large crater volumes to late-time subsidence. As the pore fluids migrate upwards through the fractured coral, the coral consolidates to a volume comparable to that attained during shock passage. This leads to surface subsidence which enlarges the early bowl-shaped transient crater. Our model also predicts shock liquefaction; liquefied coral can be expected to slump and transform a transient bowl-shaped crater into the saucer shape observed.

2. CONSTITUTIVE RELATIONSHIPS FOR MIXTURES

The constitutive model assumes a solid containing two types of flaws: pores considered to be preexisting, isotropic, and homogeneous, and cracks that are induced during the calculation and treated using an anisotropic algorithm. Although we make a logical distinction between crack and pore pressure, the assumption of pressure equilibrium between the two types of flaws reduces the system to three components (solid, water, and air). The following describes the types of relationships which govern the system response.

Kinematic Conditions. The kinematic conditions needed for a solid (s), water (w), air (a), multiphase material are

$$M_s = \rho_s (1-\phi)\, V, \quad M_w = \rho_w S \phi\, V, \quad \text{and} \quad M_a = \rho_a (1-S)\, \phi V \tag{1}$$

in which M_i is mass, ρ_i is density, V is volume, and the saturation, porosity, and the constituent porosities are defined by

$$S = \phi_w/\phi, \qquad \phi = \phi_w + \phi_a, \qquad \text{and} \qquad \phi_i = V_i/V. \tag{2}$$

Constituent Response Laws. The constituent response laws are normally given as tabular functions in terms of pressure vs density, while the low pressure water and air responses are represented by adiabatic gas law approximations,

$$\sigma_w = \sigma_w (\rho_w), \qquad \sigma_a = \sigma_a (\rho_a), \qquad \sigma_s = \sigma_s (\rho_s) \tag{3}$$

Constraints. Pressure equilibrium is assumed between the water and air and between the pores and cracks. These constraints can be recast as functions of S and ϕ or

$$\sigma_w(\phi,S) = \sigma_a(\phi,S) \quad ; \tag{4}$$

Effective Stress Law. The final volumetric relationship is provided by the effective stress law. The classical concept of effective stress is due to Terzaghi (1943) and suggests that the bulk response of a porous solid can be separated into that due to the pore fluid and that due to an "effective" stress defined as

$$\sigma_e = \sigma - \sigma_f \tag{5}$$

$$\text{with} \quad \sigma_f(\phi,S) = S\sigma_w + (1-S)\, \sigma_a. \tag{6}$$

where σ is the total stress tensor. The Terzaghi effective stress has been shown to satisfy a response law of the form [Swift 1984]

$$\dot{\sigma}_e = K \left(\dot{\varepsilon} - \frac{\dot{\sigma}_f}{K_s}\right), \tag{7}$$

where K and K_s are the drained and solid bulk moduli and $\dot{\varepsilon} = \dot{V}/V$ is the volumetric strain rate and the term in parentheses appears as an effective strain rate.

Although the effective stress response law for σ_e is convenient for purposes of understanding, it has several embedded singularities that must be removed in the numerical implementation. It was shown that the response law reduces to the following form [Swift 1984]

$$(1-\phi)\left(1-\phi - \frac{K}{K_s}\right)\left[\dot{\varepsilon} + \frac{\dot{\sigma}_f\ (S,\phi)}{K_s}\right] - \left[1 - \phi + \frac{\sigma_e\ (S,\phi)}{K_s}\right] \dot{\phi} = 0\ . \tag{8}$$

The model presently employed in the TENSOR code treats pore collapse and shear failure independently, along with tensile failure algorithms that produce volume dilatancy. In the above form the theory is reduced to solving two equations [Eqns. (4) and (8)] simultaneously for

saturation, S, and total porosity, ϕ, at each time step. This is done using a modified Newton-Raphson iteration scheme.

3. SHOCK INDUCED CONSOLIDATION

The presence of water in the coral pores profoundly affects both the transient and late-time material response and leads consolidation and liquefaction. When coral is dry it transmits shock poorly; the collapse of its pores attenuates the shock rapidly with distance, concentrating damage to the region near the source. Pores filled with water transmit shock better than air-filled pores, so the shock travels with less attenuation and can damage larger volumes of coral far from the source.

Figure 2 illustrates typical responses of drained and undrained coral. The drained coral matrix starts with an initial effective stress shown at point A. As the shock wave traverses the material, it first compresses drained coral to point B (irreversibly compacting it) and then unloads down the release path to the axis (where the coral fails in tension) and then to point C.

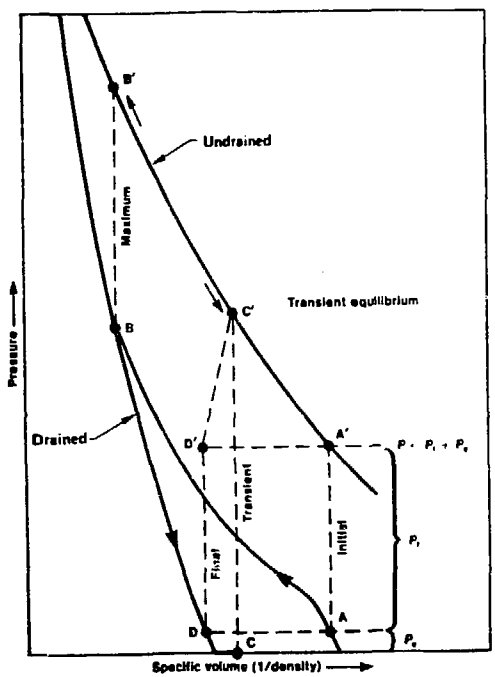

Figure 2. Curves illustrating the compaction and liquefaction processes in terms of the relationship between the responses to shock of drained and undrained coral.

The mixture theory of Section 2 enables us to describe the response of undrained coral in terms of the drained coral response at corresponding volumetric strains. For undrained coral, the shock response would be to move from point A' to the shocked condition (point B') corresponding to the strain in drained coral (point B). The corresponding degree of unloading for the undrained material is point C', at which time the material is in a transient equilibrium state with

respect to total stress. The dynamic calculation is stopped at this point.

Final equilibrium with respect to effective stress occurs by porous flow. Although we are not at present modeling porous flow, we can infer the net effects using our model by assuming that the effective stress reloads approximately back to its initial value. Because the release path BD is steep compared to BA, volume errors resulting from the effective pressure approximation are relatively small. For instance, if a calculation is stopped at point C' (corresponding to the specific volume at point C for dry coral), the net consolidation or volume change for each zone can be determined by going from point C back to point D. The final state for the system is point D'.

The surface subsidence profile is determined by adding the volume changes for all the zones vertically. We can then calculate the total volume of the subsidence crater by integrating over the subsidence profile.

4. SIMULATING THE KOA EVENT

We used the large crater produced by the Koa Event (2.11×10^7 m^3 in apparent crater volume) as a test case for our mixture model. The 1.3 Mt Koa device was detonated in a tank of water placed on a concrete pad poured over coral sand. We modeled the various layers of coral below the ground surface to a depth of 1300 m using measured densities and compressional velocities. Five types of coral were identified and the geologic profiles were obtained for the bulk density and compressional velocity as a function of depth. These profiles were constructed from density logs, core samples, and seismic velocity records.

The calculation was begun with an Eulerian code, which treats the radiation-hydrodynamic energy transfer at early times. The Eulerian code was run to a time of 1 ms and then linked to the Lagrangian code TENSOR. We mapped the pressures, densities, and velocities calculated by the Eulerian code onto a larger grid that extended to a depth of 50 m and a radius of 200 m and continued the calculations with the TENSOR code. After the link, the airblast loading on the ground surface was approximated by a pressure boundary condition due to Brode (1970). We repeated this overlay procedure six times. The final TENSOR grid extended to a depth of 1300 m and a radius of 1400 m.

Figure 3 illustrates the overlaying process, the scale of the problem, and the propagation dynamics of the ground shock. The small black square around the origin at the upper left rear represents the region depicted at early times < 1 ms. The six TENSOR grids appear arrayed along the time axis according to the times of the ground-shock pressure contours shown (2, 10, 57, 133, 280, and 500 ms). The boundaries of the final TENSOR grid extend beyond the border of the figure.

At about 45 deg from the surface, the effect of downward-traveling rarefaction waves generated by the free surface is evident in the shape of the pressure contours. The confinement of the peak pressures to a conical region about the symmetry axis is important to the subsidence interpretation that follows.

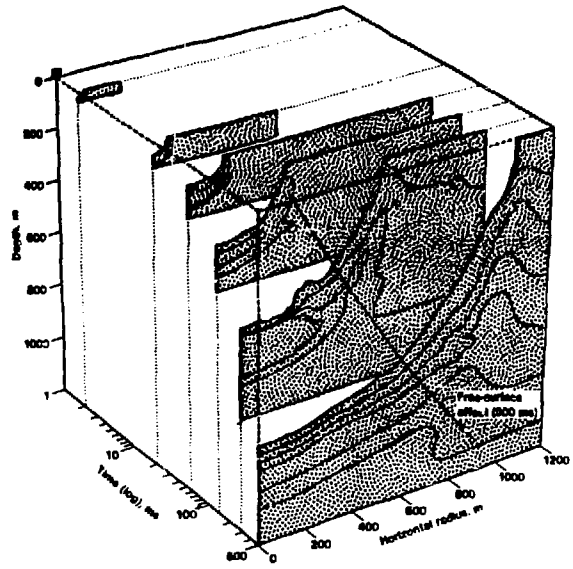

Figure 3. The complete calculation of the Koa Event, starting with the Eulerian calculation (small square at the origin of the back plane) and continuing through six successive remappings to larger grids and TENSOR calculations. Pressure contours are shown for times of 2, 20, 57, 133, 280, and 500 ms.

Figure 4 shows contours of volumetric consolidation in relation to the various coral layers in the TENSOR mesh. These contours were obtained as discussed previously, by assuming the equality of initial and final effective stress (points A and D in Fig. 2). Note that the shape of the contours corresponds to the shock-propagation contours of Fig. 3 that exhibited the strong influence of rarefaction effects off the free surface. Most of the consolidation occurred within the observed crater radius, but significant contributions occurred for the relatively porous layer at a depth between 610 and 760 m.

Figure 5 presents the Koa Event crater profile, measured along the reef, and at various phases of our calculation. The dashed curve represents the transient crater profile in the calculation at a time of 676 ms. The transient crater radius at this time was about 100 m.

Although the ground motion continues until at least 3.3 s [Schuster 1983], we terminated the calculation at 676 ms because we had carried it far enough to address the subsidence issue, which is governed primarily by the magnitude of the peak stress. We plan additional calculations out to later times, but for this study we have simply made a ballistic extrapolation to arrive at the solid profile shown in Fig. 5.

Combining our subsidence contribution with the ejecta profile, we obtain a third profile with a crater volume of 2×10^7 m^3, which is in excellent agreement with that of the actual crater, even though it has a different shape. Significant vertical displacements occur out to a radius of 500 m before rapidly tapering off.

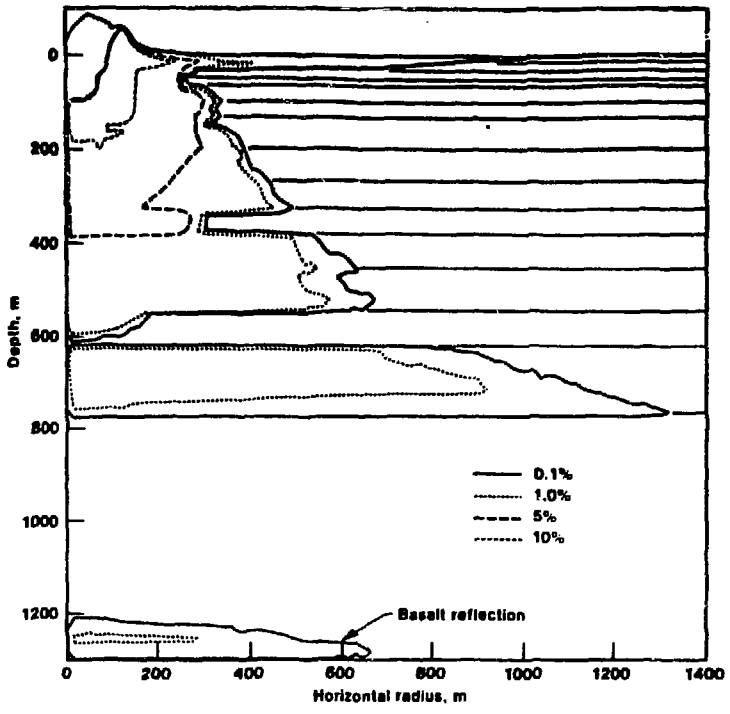

Figure 4. Consolidation contours within the various coral layers. Numbers indicate volume change in percent. The consolidation in any given zone is a function of the local porosity and the peak shock stress.

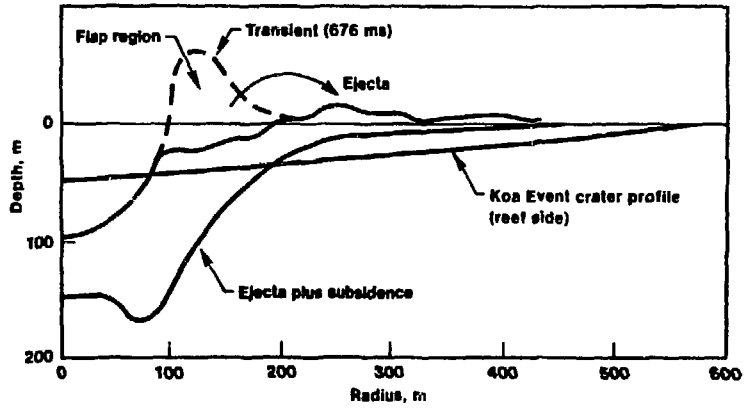

Figure 5. Actual and calculated profiles for the Koa Event crater. Long and short dashes respectively represent the calculated transient profile and the EJECT calculation of throw-out. The solid curve is the crater profile resulting from vertical subsidence, which closely matches the volume of the observed Koa Event crater.

The indicated crater shape is an artifact of assuming that the subsidence is only vertical. The constitutive model predicts that the shear strength of the liquefied material will be insufficient to support a crater of this depth, so that at some time there would be a horizontal flow that fills in the crater. We have made no attempt to model this slumping in this study, since it is the transient crater, not its final form, that is important in strategic effects. However, it does seem clear that liquifaction would rapidly transform the bowl-shaped crater into a shallow saucer like the one observed.

5. CONCLUSIONS

Based on plausible assumptions about the geology and the constitutive relations of coral, we have shown that a detailed constitutive model can relate subsidence to calculational parameters such as peak effective stress. Most of the observed volume of the Koa crater can be accounted for by late time consolidation of the damaged coral.

6. REFERENCES

Brode, H. L., "Height of Burst Effects at High Overpressures," Defense Atomic Support Agency Report DASA 2506 (1970 with 1979 update).

Burton, D. E., L. A. Lettis, Jr., J. B. Bryan, T. R. Butkovich, and A. L. Bruce, "Anisotropic Creation and Closure of Tension Induced Fractures", Lawrence Livermore National Laboratory Report, UCRL-79578, (1977).

Burton, D.E., L.A. Lettis, Jr., J. B. Bryan, and N.R. Frary, "Physics and Numerics of the TENSOR Code," Lawrence Livermore National Laboratory Rept. UCID-19428 (1982).

Burton, D.E., R.P. Swi J.B. Bryan, and H.D. Glenn, "Subsidence in the Craters of Nuclear Tests at the Pacific Proving Grounds," Lawrence Livermore Nationa Laboratory Report UCRL-91583, (1984).

Cooper, H.F. Jr., "A Summary of Explosion Cratering Phenomena Relevant to Meteor Impact Events," in Impact and Explosion Cratering, Perg mon Press (New York), D.J. Roddy, R. D. Pepin, and R.B. Merrill (eds.), (1977).

Ristvet, B. L., "Geologic and Geophysical Investigations of the Eniwetok Nuclear Craters," U.S. Air Force Weapons Laboratory, Kirtland Air Force Base, Albuquerque, NM, Rept. AFWL-TR-77-242, (1978)

Schuster, S.H., and V. E. Koit, "Initial KOA Calculations," Seventh Meeting of the DNA Ad Hoc Cratering Working Group, R&D Associates, Marina del Rey, CA, November (1983).

Swift, R.P., and D. E. Burton, "Numerical Modeling of the Mechanics of Non-linear Porous Media Under Dynamic Loading," Lawrence Livermore National Laboratory Report UCRL-53568 (1984).

Terzaghi, K., Theoretical Soil Mechanics, Wiley, New York, (1943).